농학석사학위논문

Functional characterization of genes encoding putative nuclear movement and positioning - associated proteins in *Magnaporthe oryzae*

벼 도열병균에서 핵 이동과 고정에 관여하는 유전자들의 기능분석

2013년 2월

서울대학교 대학원

협동과정 농업생물공학전공

노 희 경

A THESIS FOR THE DEGREE OF MASTER OF SCIENCE

Functional characterization of genes encoding putative nuclear movement and positioning - associated proteins in *Magnaporthe oryzae*

BY

Heekyung Roh

Interdisciplinary Program In Agriculture Biotechnology

The Graduate School of Seoul National University

February 2013

ABSTRACT

Functional characterization of genes encoding putative nuclear movement and positioning - associated proteins in *Magnaporthe oryzae*

Heekyung Roh

Interdisciplinary Program

In Agricultural Biotechnology

The Graduate School of Seoul National University

Rice blast pathogen, *Magnaporthe oryzae*, causes serious damage to global rice production and has been emerged as a model organism for the characterization of molecular mechanisms relevant to pathogenic development in host plants. Nuclei migration and distribution are known as important processes in development of infection structures called appressorium in *M. oryzae*. Two genes homologous to *ApsA* and *ApsB*

in *Aspergillus nidulans* were selected to understand nuclear migration in *M.oryzae*. In *A. nidulans,* ApsA and ApsB proteins are involved in the regulation of asexual reproduction and *apsA* and *apsB* deletion mutants showed defects in nuclear migration and positioning of the fungus.(Veith *et al.*, 2005) However, little is known about the molecular mechanisms involved in nuclear distribution during conidiation in *M. oryzae*. Two genes were named Abnormal Nuclear Distribution (*MoAND1* and *MoAND2*, respectively) and gene deletion mutant of *MoAND1* was obtained by mycelial growth and conidiation. Observation of nuclei and septa after staining with Hoest33342 and Calcofluor White indicated that the Δ*Moand1* mutant produced abnormal conidia such as one-, two-, four-, and five-celled conidia compared to three-celled wild-type conidia. To elucidate nuclei movement and positioning, RFP-tagged histones were introduced into both wild-type and Δ*Moand1* strains. Microscopic observation of the Δ*Moand1* strains with RFP-tagged histones revealed that nuclei distributed unevenly in hyphae and even some cells had no nucleus. Pathogenicity of Δ*Moand1* was significantly reduced and this might be due to defects of appressorium formation and invasive growth in host cells. Furthermore, Δ*Moand1* and double KO strain of *MoAND1* and *MoAND2* were more sensitive to microtubule-depolymerizing agent Benomyl, indicating that the mutants are

defective in microtubule function. Taken together, these results represent that MoAND1 and MoAND2 are essential for pathogenicity as well as nuclei distribution in *M. oryzae*.

KEYWORDS: *Magnaporthe oryzae*, nuclear movement, nuclear positioning

Student number:2011-21275

CONTENTS

LIST OF TABLES

page

LIST OF FIGURES

page

INTRODUCTION

In eukaryotic cells, nuclear movement and distribution are essential for survival. For this, exact nuclear positioning with regards to time and space is crucial for developmental processes. A well-known example is nuclear division and subsequent migration in the case of *Saccharomyces cerevisiae.* In *S. cerevisiae,* nuclei migrate to the budding neck before a localized mitosis, providing bud and mother cell with a nucleus (Brachat *et al.*, 1998). Several components have been shown to be involved in nuclear migration such as Num1. A role of Num1 protein is related positioning of the G2 nucleus at the budding neck of a dividing yeast cell. Nuclear movement has also been described in cells of mammals during embryogenesis(Reeve & Kelly, 1983). Nuclear migration is especially important in longitudinal elongated cells that grow by apical extension like filamentous fungi. The species that are studied well are *A. nidulans*. In this, nuclei migrates long distance during hyphal growth. The analyses of the specific nuclear movement genes have been described. ApsA and ApsB, which are homologous to NUM1 protein in *S. cerevisiae,* display an aberrant nuclear distribution phenotype when mutant (Veith et al., 2005). In these mutants, nuclei are not evenly distributed in hyphae in contrast to wild-type.

Therefore, nuclei are clustered and some areas lack any nuclei. In addition to this hyphal phenotype, the aps mutants severely affect conidiophore development.

In *Magnaporthe oryzae*, nuclei migration and positioning are also important for pathogenicity. After conidial attachment to host tissues, a germ tube emerges at the conidial apex, elongates for a brief period, with a limited number of cell divisions, and arrests polar growth upon sensing host signals. The tip of a germ tube differentiates the dome-shaped appressorium, which enables the fungus to penetrate host barriers through turgor pressure-mediated mechanical disruption. For appressoria morphogenesis, it has been studied that mitosis consistently occurred within germ tube before appressorium development (Veneault-Fourrey *et al.,* 2006). Moreover, appressorium development in *M. oryzae* involves spatial uncoupling of mitosis and cytokinesis. The cell division that leads to appressorium differentiation is defined initially by formation of a heteromeric sptin ring complex before onset of mitosis(Saunders *et al.*, 2010). After appressoirum formation, the appressorial nucleus migrated to the penetration hyphae and underwent mitosis before the development of the invasive hypha. However, the details of these mechanisms are still almost completely unknown in *M. oryzae*. A key to understanding nuclear movement is the identification and

characterization of nuclear movement proteins. To understand nuclear movement mechanisms in *M. oryzae*, we report that two related genes named *MoAND1* and *MoAND2* (from Abnormal Nuclear Distribution) encodes proteins MoAND1 and MoAND2 that functions as microtubules polymerization of *M. oryzae*. To unveil the functional roles of *MoAND1* and *MoAND2*, a gene deletion mutant was generated using a targeted gene replacement strategy. In *M. oryzae*, the function of *MoAND1* was related nuclear migration and distribution. However, unlike other homologous organisms, Δ*Moand1* represented severely affected conidia morphology which showed increased or decreased number of nuclei and septa. Most importantly, *MoAND1* was required for asexual development and pathogenicity, the most important means for dispersal and survival through infectious propagules of plant pathogen. These results suggest that the functions of *MoAND1* and *MoAND2* homologs have been adapted to different patterns of growth through eukaryotic evolution.

MATERIALS AND METHODS

I. Fungal strains and culture conditions

M. oryzae wild-type strain KJ201 and gene disrupted strains ATMT mutants used in this study were obtained from the Center for Fungal Genetic Resources (CFGR, http://genebank.snu.ac.kr). Other strains generated in this study were stored in the CFGR. The strain and its transformants were steadily maintained on oatmeal agar media (OMA, 5% oat meal (w/v), 2.5% agar powder (w/v)) or V8 juice agar media (8% V8 juice (w/v), 1.5% agar powder (w/v), pH6.7) at 25℃ under the constant fluorescent light. Hygromycin-resistant transformants were selected using TB3 agar media (0.3 % yeast extract (w/v), 0.3% casamino acids (w/v), 1% glucose (w/v), 20% sucrose (w/v) and 0.8% agar powder (w/v)) supplemented with hygromycin B (200 ppm final concentration). Mycelia of the strain and its transformants were used for genomic DNA and RNA extraction, that cultured on liquid complete media (LCM, 0.6% yeast extract (w/v), 0.6% casamino acid (w/v) and 1% sucrose (w/v)) at 25℃ with agitation (150-200rpm). To observe their developmental and morphologic phenotypes and pathogenicity ability, they cultured on V8 juice agar media for 7 days or on OMA for 10 to 15 days at 25℃ under the continuous light condition.

II. Sequence analysis

Nucleotide and protein sequences were taken and analyzed by using the computer programs provided at the Comparative Fungal Genomics Platform ((Park *et al.*, 2008), http://cfgp.snu.ac.kr/) and the Blast program provided at the National Center for Biotechnology Information, Bethesda, USA (http://www.ncbi.nlm. nih.gov/blast/) (McGinnis & Madden, 2004). Sequences were aligned by ClustalW algorithm (Thompson *et al.*, 1994) and phylogenetic trees were designed using the neighbor-joining method at the MEGA 5.0 program. Domain architectures were drawn by using InterProScan (Mulder *et al.*, 2005).

III. Nucleic acid manipulation

Genomic DNA extraction was performed with two different processes in accordance with the purpose. Genomic DNA for PCR-screening was extracted by quick and convenient method (Chi *et al.*, 2009). Genomic DNA isolated by standard process was used to other general experiments such as restriction enzyme digestion and Southern hybridization analysis (Rogers & Bendich, 1985). Agarose gel separation, restriction enzyme digestion and Southern hybridization analysis were performed following standard procedures (Sambrook *et al.*, 1989). DNA fragments for

DNA hybridization probes were labeled with ^{32}P by using Rediprime™ II Random Prime Labeling System kit (Amersham Pharmacia Biotech, Piscataway, NJ, USA) according to the manufacturer's manuals. Total RNA for expression analysis was extracted by using the Easy-Spin™ total RNA extraction kit (Intron Biotechnology, Seongnam, Korea) according to the manufacturer's instruction. To perform the expression analysis by quantitative real-time PCR (qRT-PCR), 5μg of total RNA was used and cDNA synthesis was performed using the oligo dT primer with the ImProm-II™ Reverse Transcription System kit (Promega, Madison, WI, USA) following the manufacturer's instruction.

IV. Construction of the *MoAND1* deletion mutants and complemented mutants

The gene deletion mutants were generated via the homologous recombination. Shortly, the knock-out constructs composed of 1.4Kb of hygromycin B phosphotranferase (*HPH*) cassettes fused with ~1 Kb 5'- and 3'- flanking regions were replaced with the original sequences of MGG_02961 (Yu, Hamari et al. 2004). Hygromycin-resistant transformants were selected on media supplemented with hygromycin B and screened by PCR with primers (Table 2). One mutant candidate for MGG_02961 was

found and confirmed by Southern blot analysis (Fig. 3). Complemented mutants were generated following the similar procedures. A fragment carrying the ORF sequence for complementation was amplified from KJ201 genomic DNA. The ORF fragment and geneticin fragment from pII9 were co-transformed in each deletion mutant protoplasts from Δ*Moand1*. Complemented mutants were selected on media supplemented with geneticin and screened through the phenotype assay.

V. Fungal developmental assay – Mycelial growth, conidiation, conidial morphology, conidial germination and appressorium formation

Mycelial growth was measured with their diameter of each three replicates on minimal agar media and Talbot modified complete agar media (TCM) every three days by 9 days after inoculation. The used inoculums were from 6-day-old minimal agar media (MM) (Talbot *et al.*, 1993). Conidiation was measured by counting the number of asexual spores within 10μl conidia suspension onto hemacytometer under a microscope. Conidia was collected from 7-day-old V8 juice agar plates with 5ml sterilized distilled water. Conidial morphology was observed under a microscope and the sizes of conidia were measured as their width and length. Conidial germination and appressorium formation were performed on hydrophobic

microscope coverslips. Conidia used this assay was harvested from 7-day-old V8 juice agar plates or 10-day-old OMA plates and passed through the two layer mira cloth with sterilized distilled water. Conidia suspension adjusted to $2X10^4$ conidia per millimeter was dropped onto coverslips with three replicates and incubated in moistened box at room temperature. Each two and four hours after incubation, germination rate was determined within at least a hundred of conidia per replicate under a microscope. The rate of appressorium formation was determined within the percentage of germinated conidia at 8 and 16 hours each after incubation. These assay processes were performed with three replicates in three independent experiments.

VI. Conidiogenesis assay

Conidiogenesis assay was performed with scraped mycelia agar plugs from 20-day-old OMA plates. Coverslips were placed on scraped mycelia agar plugs and they were incubated in moistened box for 24, 36 and 42 hours at room temperature. Conidiophore development was monitored under a microscope at the times after incubation (Lau & Hamer, 1998).

VII. Pathogenicity and leaf sheath injection

For the pathogenicity assay by spray inoculation, conidia were collected

from 7-day-old V8 juice agar media and 10 ml of filtered conidia suspension adjusted to $5X10^4$ conidia per millimeter containing Tween 20 (250 ppm final concentration) was sprayed onto the rice seedlings (*Oryza sativa* cv. Nakdongbyeo) in three to four leaf stage. Inoculated rice seedlings were placed in a dew chamber for 24 hours under the dark condition at 25℃. After then, they were transferred to the rice growth incubator maintained 25℃, 80% humidity and with photoperiod of 16 hours with fluorescent lights (Valent *et al.*, 1991). Drops of conidia suspension (10^5 cells per milliliter final concentration) and mycelia agar plugs were used for the pathogenicity assay as well. The detached rice leaves were infected with 20 μl of drops of conidia suspension or 6 mm mycelia agar plugs and incubated in moistened box for seven days at room temperature (Kim *et al.*, 2009).

For the leaf sheath injection, filtered conidia suspension adjusted to $2X10^4$ conidia per millimeter and rice sheath of four to six leaf stage were used (Koga *et al.*, 2004). Conidia suspension was injected in excised rice sheaths and incubated in moistened box for 48 and 72 hours at room temperature. After incubation, the infected rice sheaths were trimmed to remove chlorophyll enriched plant parts. Left epidermal layers of mid vein (three to four cell layers thick) were used for microscopic experiment.

VIII. Expression profiling of *MoAND1 and MoAND2*

To analyze the expression of *MoAND1* and *MoAND2* in over-expression strains, mycelia of the strains were treated following the process. Mycelia of each over-expression strain was cultured on CM liquid media for 4 days and collected onto two layers of miracloth with washing by sterilized distilled water. RNA extraction and cDNA synthesis from mycelia of the strains were performed following previously described procedures. Quantitative real-time PCR (qRT-PCR) reactions were performed in 10 µl solution containing 2 µl of cDNA template (12.5 ng/ µl), 3 µl of forward and reverse primers (100 nM concentration for each) and 5 µl of Power SYBR® Green PCR Master Mix (Applied Biosystems, Foster city, CA, USA). Samples were run for 40 cycles of 15 s at 95℃, 30 s at 60℃ and 30 s at 72℃ after 3 m of denaturation at 95℃ on AB7500 Real-Time PCR system (Applied Biosystems). To compare the relative abundance of *MoCOD1* transcripts, the average of threshold cycle (Ct) was normalized to that of *β-tubulin* gene for each of the treated samples as $2^{-\Delta\Delta Ct}$, where $-\Delta\Delta Ct = (C_{t,\ target\ gene} - C_{t,\ \beta\text{-tubulin}})_{test\ condition} - (C_{t,\ WT} - C_{t,\ \beta\text{-tubulin}})_{CM}$ (Choi *et al.*, 2009).

RESULTS

Ⅰ. Identification of two genes involved in nuclear migration and distribution *Magnaporthe oryzae*.

To understand nuclear migration and distribution in *M. oryzae*, two genes MGG_02961 and MGG_10857, homologous to ApsA and ApsB in *Aspergillus nidulans* were selected and named MoAND1 and MoAND2 (Abnormal Nuclear Distribution). BLAST analysis (blastp) was performed to identify homologues in other fungi using NCBI web site. Four genes and three genes have functionally characterized homologues for MGG_02961 and MGG_10857, respectively.

Bioinformatic analysis for MGG_02961.6 and MGG_10857.6 was performed. The MGG_02961.6 gene was predicted to have both the Pleckstrin homology domain (Fig. 1. yellow box) in N-terminal region and coil-coil motif (Fig. 1. green box) in C-terminal region. The MGG_10857.6 gene was contained Spindle-associated domain and coiled-coil motif. BLAST searches were carried out for genes homologous to the ORFs of MGG_02961.6 and MGG_10857.6. MGG_02961 showed high similarity to ApsA in *Aspergillus nidulans* and to Ami1 in *Podospora anserine*.

MGG_10857.6 also showed similarity to Mcp6 in *S. pombe*. ApsA which is MGG_02961.6 homologue in *A. nidulans*, has so far been implicated in nuclear distribution and positioning in hyphae. ApsB also has been revealed to relate nuclear distribution and migration.

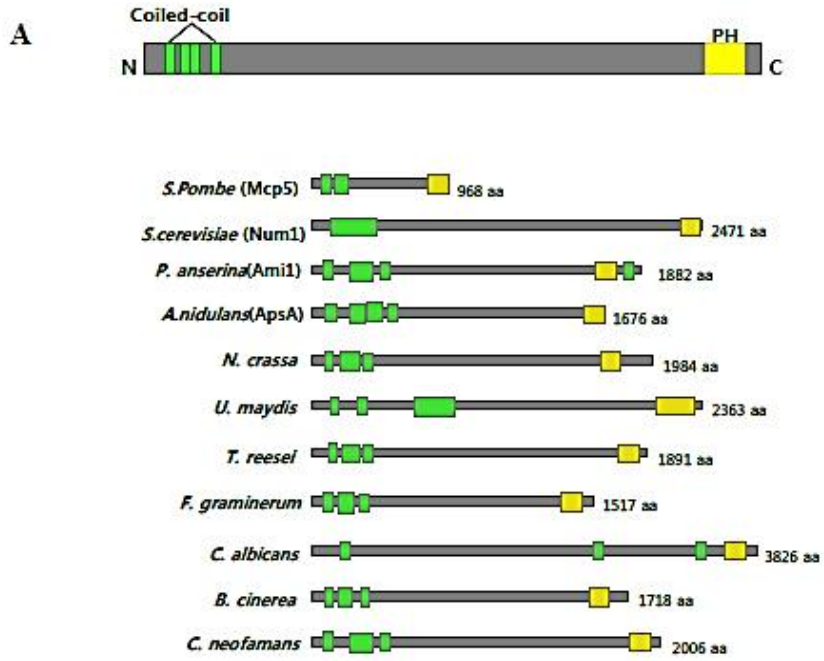
A
Coiled-coil
PH
N
C
S.Pombe (Mcp5)
968 aa
S.cerevisiae (Num1)
2471 aa
P. anserina(Ami1)
1882 aa
A.nidulans(ApsA)
1676 aa
N. crassa
1984 aa
U. maydis
2363 aa
T. reesei
1891 aa
F. graminerum
1517 aa
C. albicans
3826 aa
B. cinerea
1718 aa
C. neofamans
2006 aa


B

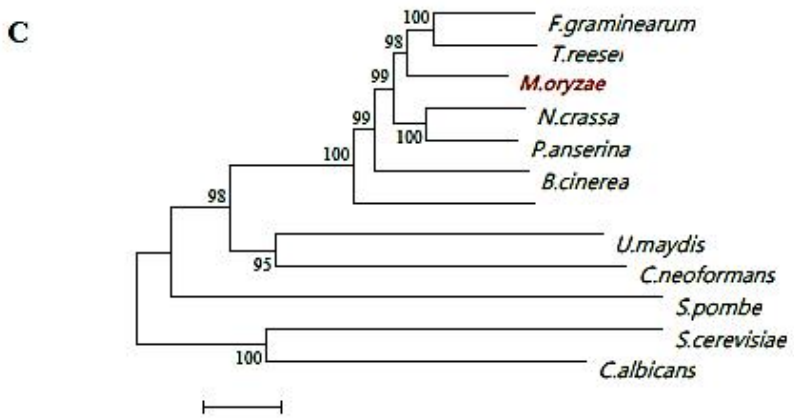
C
100
98
99
99
100
100
98
95
100
F.graminearum
T.reesei
M.oryzae
N.crassa
P.anserina
B.cinerea
U.maydis
C.neoformans
S.pombe
S.cerevisiae
C.albicans

Figure 1. *MoAND1* is a coiled-coil protein that belongs to the ApsA family proteins found specifically among fungi.

(A) Schematic representation of *MoAND1* and the *ApsA* family proteins. The location of the coiled-coil motif (green) and the PH domain (yellow) are indicated. These motifs were identified by PSORT II (http://ch.EMBnet.org/) and (http://**smart**.embl-heidelberg.de/).

(B) NH2-terminal half residues of PH domains with And1 orthologs were aligned. Gaps inserted in the alignment to attain maximal homology are indicated by hyphens. The color of blue or light blue indicated amino acids those are identical or similar among 12 species.

(C) The phylogenetic tree of ORF from *MoAND1* orthologous proteins. The relationships between the sequences were inferred by the Neighbour-Jonining method. The length of the horizontal lines represents the phylogenetic distance. Both the sequence and phylogenetic analyses were performed by using a MEGA program.

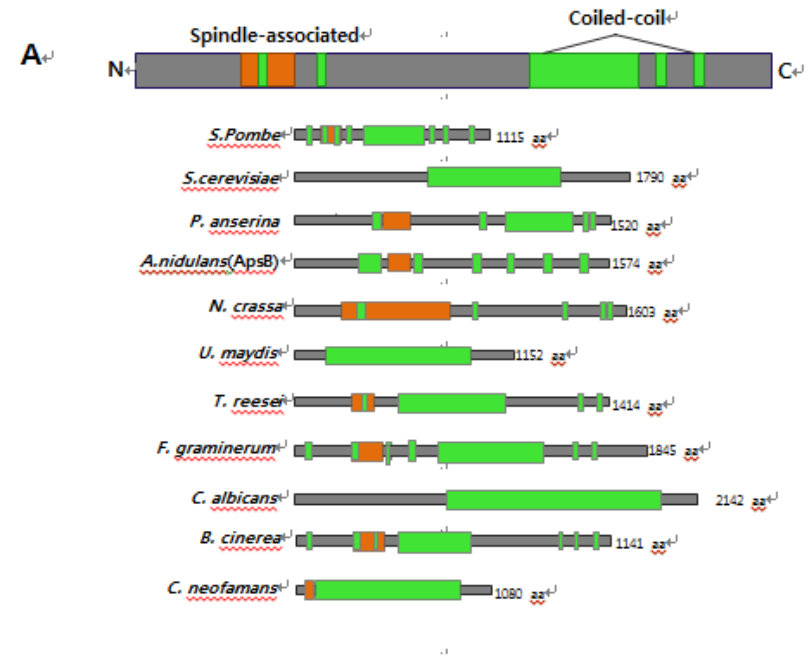
A
Spindle-associated
Coiled-coil
N
C
S.Pombe 1115 aa
S.cerevisiae 1790 aa
P. anserina 1520 aa
A.nidulans(ApsB) 1574 aa
N. crassa 1603 aa
U. maydis 1152 aa
T. reesei 1414 aa
F. graminerum 1845 aa
C. albicans 2142 aa
B. cinerea 1141 aa
C. neofamans 1080 aa

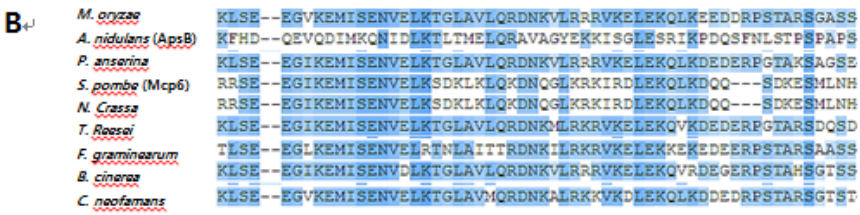
B
M. oryzae KLSE--EGVKEMISENVELKTGLAVLQRDNKVLRRRVKELEKQLKEEDDRPSTARSGASS
A. nidulans (ApsB) KFHD--QEVQDIMKQNIDLKTLTMELQRAVAGYEKKISGLESRIKPDQSFNLSTPSPAPS
P. anserina KLSE--EGIKEMISENVELKTGLAVLQRDNKVLRRRVKELEKQLKDEDERPGTAKSAGSE
S. pombe (Mcp6) RRSE--EGIKEMISENVELKSDKLKLQKDNQGLKRKIRDLEKQLKDQQ---SDKESMLNH
N. Crassa RRSE--EGIKEMISENVELKSDKLKLQKDNQGLKRKIRDLEKQLKDQQ---SDKESMLNH
T. Reesei KLSE--EGIKEMISENVELKTGLAVLQRDNKMLRKRVKELEKQVKDEDERPGTARSDQSD
F. graminearum TLSE--EGLKEMISENVELRTNLAITTRDNKILRKRVKELEKKEKEDEERPSTARSAASS
B. cinerea KLSE--EGIKEMISENVDLKTGLAVLQRDNKVLRRRVKELEKQVRDEGERPSTAHSGTSS
C. neofamans KLSE--EGVKEMISENVELKTGLAVMQRDNKALRKKVKDLEKQLKDDEDRPSTARSGTST

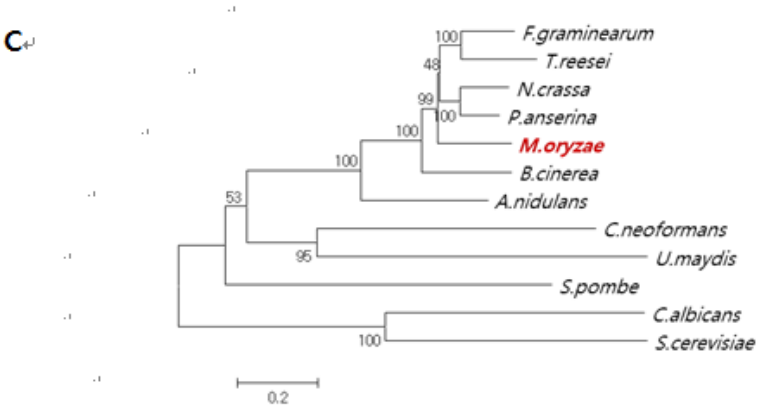
C
F.graminearum
T.reesei
N.crassa
P.anserina
M.oryzae
B.cinerea
A.nidulans
C.neoformans
U.maydis
S.pombe
C.albicans
S.cerevisiae
100
48
99
100
100
100
53
95
100
0.2

Figure 2. *MoAND2* is a coiled-coil protein that belongs to the ApsB family proteins found specifically among fungi.

(A) Schematic representation of *MoAND2* and the ApsB family proteins. The location of the coiled-coil motif (green) and the Spindle-associated domain (red) are indicated. These motifs were identified by PSORT II (http://ch.EMBnet.org/) and (http://smart.embl-heidelberg.de/).

(B) Spindle-associated domains with *MoAND2* orthologous were aligned. Gaps inserted in the alignment to attain maximal homology are indicated by hyphens. The color of blue or light blue indicated amino acids those are identical or similar among 9 species.

(C) The phylogenetic tree of ORF from *MoAND2* orthologous proteins. The relationships between the sequences were inferred by the Neighbour-Jonining method. The length of the horizontal lines represents the phylogenetic distance. Both the sequence and phylogenetic analyses were performed by using a MEGA program.

Ⅱ. Targeted gene replacement of AND1 gene in *M. oryzae*

To characterize the function of MGG_02961.6 in *M. oryzae*, gene deletion vector was constructed by double joint PCR (Yu *et al.*, 2004), in which the hygromycin resistance gene (HPH) cassette was combined with flanking regions (Fig. 3). This construct was introduced to wild-type KJ201 protoplast by PEG-mediated fungal transformation. One mutant was generated and confirmed by Southern hybridization using 5' flanking region as a probe (Fig. 3). The functional complementation for the mutant was done. The fragment amplified using UF/DR primers form the KJ201 genomic DNA was co-transformed with a geneticin resistance gene fragment into protoplasts of mutants. Functional complement transformants were confirmed by phenotype recovery. The Δ*Moand1* mutant exhibited indistinguishable phenotypes. The Δ*Moand1* mutant defects in conidia morphology, conidial germination, appressorium formation and mycelial growth on both complement and minimal agar media.

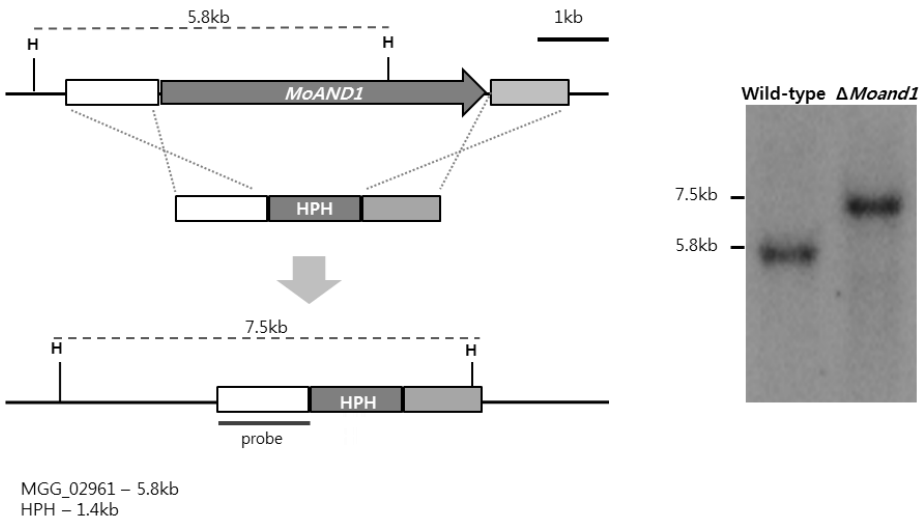

Figure 3. Targeted gene replacement of *MoAND1* gene in *M. oryzae*.

Schematic diagram of targeted gene replacement. *MoAND1* gene ORF (arrow) was replaced with *HPH* cassette. Restriction enzyme site and flanking region (white and light gray box) is shown above the lines representing genomic regions spanning target loci. To confirm the deletion mutants, Southern hybridization was performed. Each band size was identified using flanking region as probe.

Ⅲ. Expression analysis of MoAND1 and MoAND2

Expression levels of MGG_02961.6 and MGG_10857 in developmental stages were examined by quantitative real-time PCR (qRT-PCR). Total RNA samples were prepared for the four different stages in *M. oryzae* strain KJ201: mycelial growth, conidiation, germination and appressrium formation (Fig. 4). Expression of each sample of development stages was calculated compared to that of germinating conidia. The expression of MGG_02961 was increased by 1, 0.8 and 0.7-fold in mycelial growth, conidiation and appressorium formation, respectively. Expression of MGG_10857.6 was highly up-regulated in conidiation by 23.3-fold. From these qRT-PCR results, it was expected that MGG_02961.6 might be involved in mycelial growth along with conidiation and appressorim formation, and MGG_10857.6 gene might be related to conidia development alone.

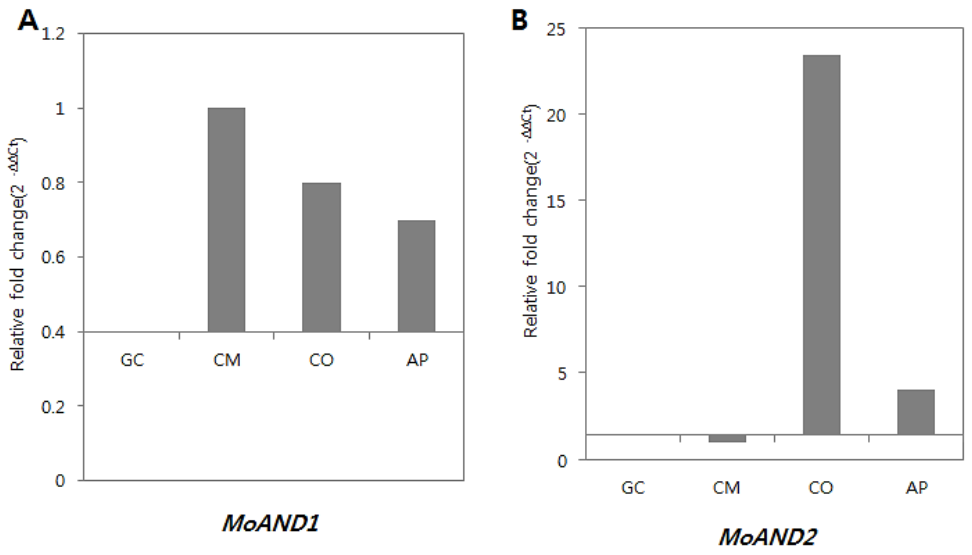

Figure 4. Expression of *MoAND1* and *MoAND2* in developmental stages.

Transcript levels of *MoAND1* and *MoAND2* during developmental stages in *M. oryzae*. (A) Relative expression of *MoAND1* gene during mycelial growth. Transcript expression was quantified by qRT-PCR analysis and values were normalized to expression of *β*-tubulin. Relative expression levels, presented as fold changes ($2^{-\Delta\Delta C}$), were calculated by comparison with wild-type strain.

(B) Relative expression of *MoAND2* gene during mycelial growth. Calculations were performed as described in (A).

Ⅳ. *MoAND1* is involved in hyphal growth, conidial shape and septum formation

To find out the functions of *MoAND1* in hyphal growth, conidial shape and septum formation, conidia was harvested from 10-day-old OMA cultures. Mycelial growth of the Δ*Moand1* mutant was somewhat impaired on complete medium and was more severely impaired on minimal media, in comparison with the wild-type strain (Fig. 7). However, this growth defect was rescued in the Moand1c strain, in which mycelial growth was similar to the wild-type. Conidia shape was severely affected by *MoAND1* deletion mutant (Fig. 5). In wild-type, three-cell conidia are appeared with a nuclear in each cell. However, in Δ*Moand1*, a large number of one-, two-, four-, and five-celled conidia were produced. Hoest33342 staining revealed that some conidia cells abnormally had several nuclei in a cell and empty cells also appeared. To assess whether impaired growth of the Δ*Moand1* mutant was associated with defects in septation during hyphal growth, we stained hyphae of each strain with calcofluor white to better visualize septa. As shown in Figure. 5, hyphae in Δ*Moand1* mutant appeared to contain an increased number of septa, resulting in the formation of hyphal compartments shorter in length. These data indicated that *MoAND1* was required for proper conidia morphology as well as hyphal growth in *M. oryzae*.

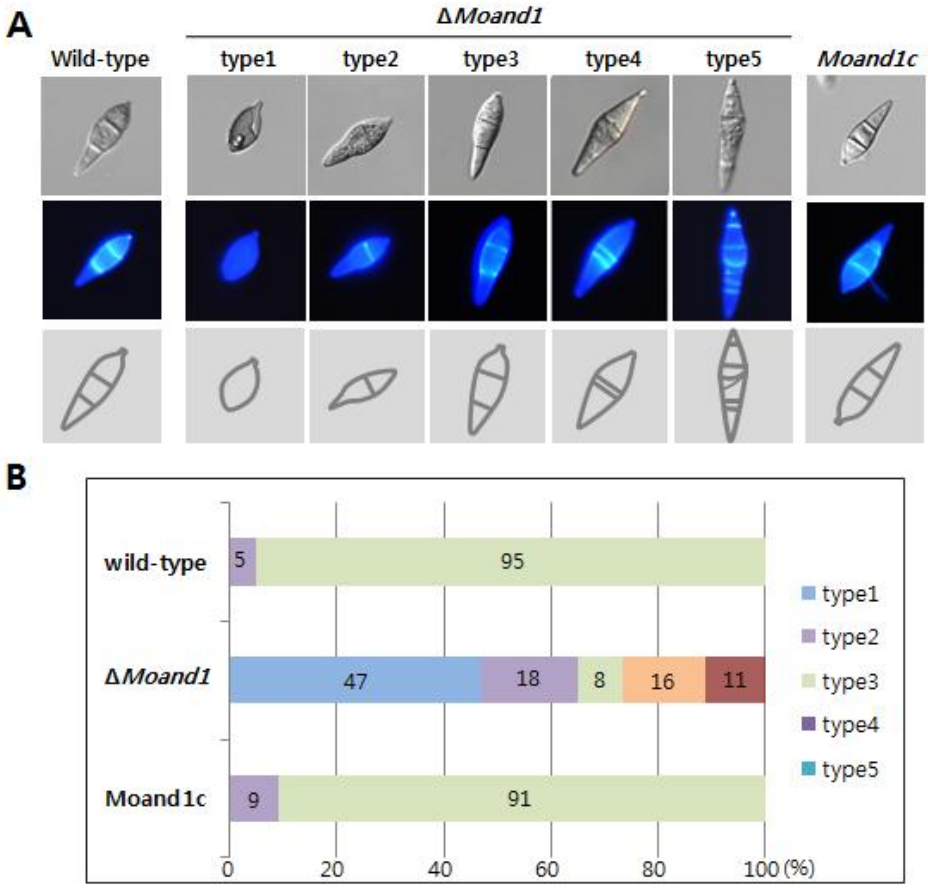

Figure 5. Effect of *MoAND1* deletion on conidial morphology of *M. oryzae*.

(A) Conidial shape and septum formation was analyzed *in M. oryzae* wild type, Δ*Moand1*, and Moand1c strains. Conidia obtained from 7-day-old cultures grown on oatmeal agar plates were stained with calcofluor white and observed either under a light microscope (upper) or under UV (down).

(B) Distribution of conidia cell numbers in control and *ΔMoand1* mutant strains.

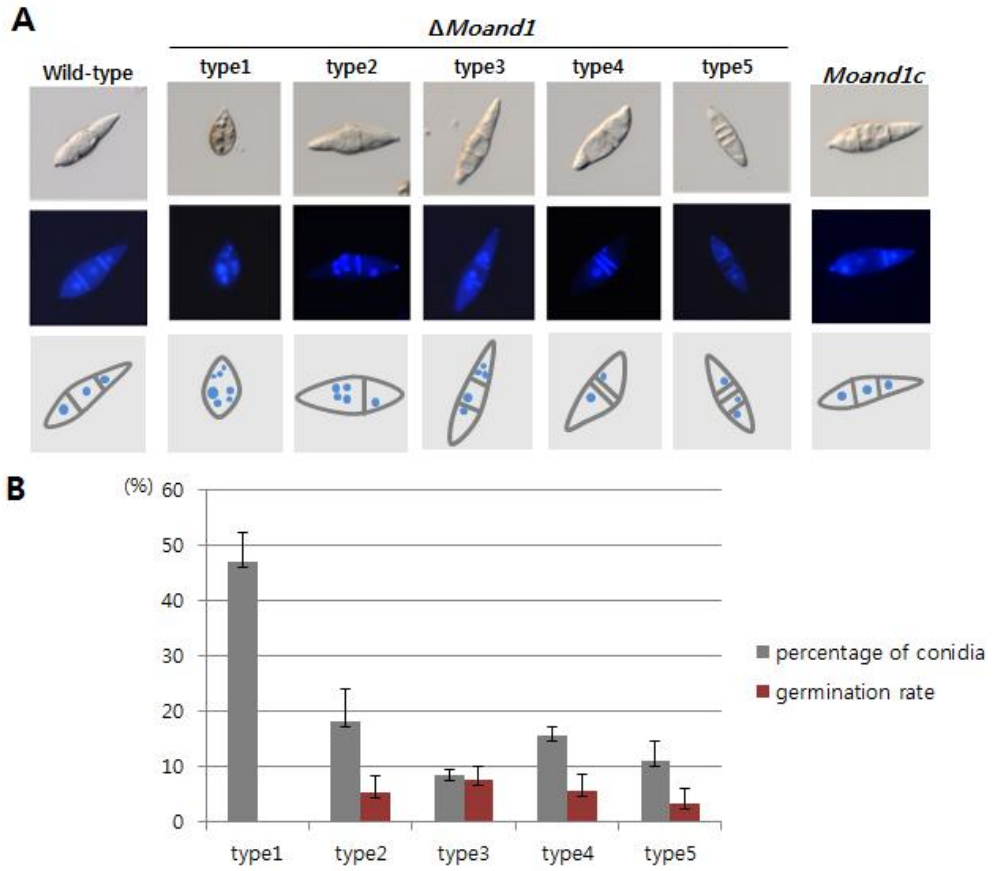

Figure 6. Effect of *MoAND1* deletion on nuclear distribution in *M. oryzae* conidia.

(A) Conidial shape and the number of nuclei were analyzed in both Δ*Moand1* and Wild-type. Conidia obtained from 7-day-old cultures grown on oatmeal agar plates were stained with Hoest 33342 to visualize nuclei and observed either under a light microscope (upper) or under UV (middle). Five conidia of Δ*Moand1* indicated representative morphology of mutant conidia.

(B) Germination rate of each conidia type was measured.

Ⅴ. *MoAND1* is involved in conidiophore development and conidial production.

To assess the functions of *MoAND1* in conidiation, conidial production was measured quantitatively by harvesting conidia from 10-day-old OMA cultures. As shown in Figure.7, conidial production was significantly reduced in Δ*Moand1* mutant, compared with the wild-type strain.

However, this defect in conidial production was fully rescued, to wild-type levels, by complementation with *MoAND1* in the Δ*Moand1* strain. To better characterize the effects of *MoAND1* deletion on conidial formation, microscopic observation was performed (Fig.7). This analysis revealed that the wild-type strain formed dense conidiophores bearing pear-shaped conidia in a sympodial pattern, while the Δ*Moand1* strain produced very few conidiophores, primarily consisting of one conidium or a couple of conidia in a chain. These result indicated that *MoAND1* was required for both conidiophore and conidium development.

A

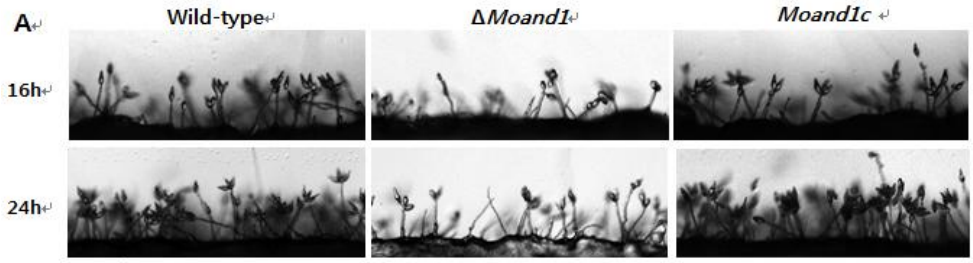

B

Strain	Conidiation (10^5/ml)	Germination (%)	Appressorium formation(%)	Growth (mm)	
				CMA	MMA
Wild-type	4.5 ± 0.4	95.7 ± 3.4	93.3 ± 2.5	52 ± 0	44 ± 0.5
Δ*Moand1*	1.6 ± 0.2	38.0 ± 9.1	39.7 ± 8.4	49 ± 0.2	42 ± 0.5
Moand1c	4.1 ± 0.2	93.3 ± 1.7	97.1 ± 1.1	52 ± 0	45 ± 0.1

Figure 7. Conidia development of *MoAND1*.

(A) Conidia and conidiophore development of Δ*Moand1* were observed at 16 and 24 hours after incubation. Light microscopic images of conidia and conidiophore development from 10-day-old oatmeal agar block.

(B) Number of conidia harvested from 10-days-old cultures on oatmeal agar plates. Percentages of appressorium formation among germinated conidia were measured on a hydrophobic surface after 24h.

Ⅵ. Nuclear distribution in hyphae and appressorium

Histone 1: RFP (red fluorescent protein) gene fusion was introduced into both wild-type strain and *MoAND1* deletion mutant strain of *M. oryzae* to observe nuclei movement and distribution. Microscopic observation of H1: RFP indicated that a *MoAND1* mutant is defective in nuclear distribution in hyphae. Clusters of nuclei (Fig. 8) are separated by large gaps without nuclear in a cell in mutant hyphae. In merge image with calcofluor white, red arrow showed two nuclei in a cell and green arrows represent empty cells without nuclear.

Moreover, conidial germination and appressorium formation were observed on a hydrophobic surface for Δ*Moand1* mutant and its complemented strains (Fig. 7). At four hours after incubation, 95% of wild-type conidia germinated, while only 38% of conidia developed germ tubes in Δ*Moand1* mutant, (Fig. 7). More than 93% of wild-type conidia formed melanized appressorium at the end of conidial germ tube within eight hours after incubation. At the same time, only 35% of Δ*Moand1* conidia formed appressorium. Δ*Moand1* conidia formed a germ tube and appressorium developed a second germ tube and appressoirum at the same or opposite orientation, and subsequently a third, having total of three

appressoria (Fig. 9). At 24h, 22% of conidia from Δ*Moand1* possessed two appressoria; these percentages became 26% at 48h. A small percentage of Δ*Moand1* conidia formed a third appressorium after germination. Nuclear distribution of the conidia producing two or three appressorium was observed using histone-tagged RFP strains. In multiple appressoriua, nuclei were distributed abnormally as shown Fig. 9. In wild-type strain, one nuclear was distributed at a appressoria but two or three nuclei was located near appressoria or in appressoria in Δ*Moand1* conidia. Such multiple formation of appressorium in Δ*Moand1* mutant was markedly recovered in Moand1c. This result indicated that *MoAND1* is important for correct development of the germ tube and appressorium by regulating nuclear migration and positioning in *M. oryzae*.

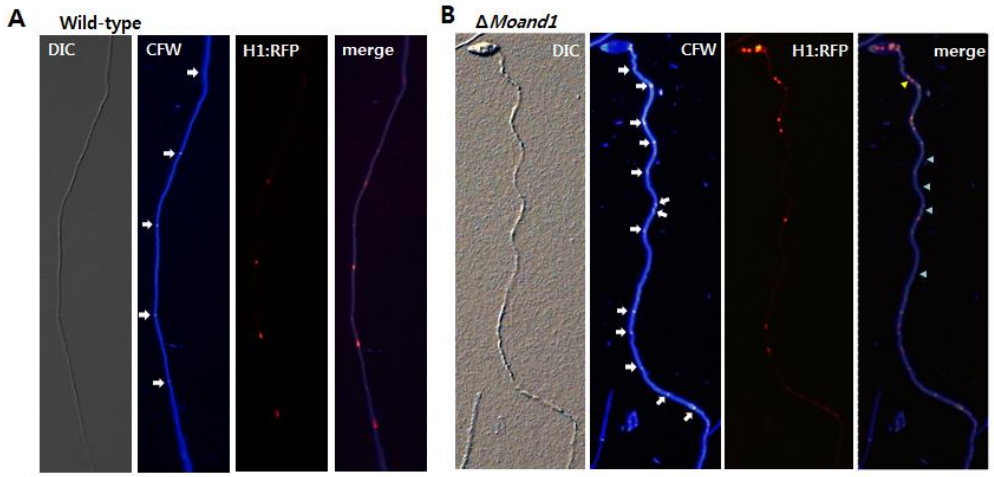

Figure 8. Nuclear distribution in hyphae of wild-type and MoAND1 deletion mutant.

(A) Nuclei and septa distribution were analyzed in Wild-type. Conidia obtained from 10-day-old cultures grown on oatmeal agar plates. Nuclei in wild-type hyphae are evenly distributed. Nuclei were visualized by constructing H1:RFP gene fusions in *M. oryzea*.

(B) Nuclei and septa distribution were analyzed in Δ*Moand1*. White arrow indicated septa. Clusters of nuclei (red arrow) are separated by large gaps (green arrow) in mutant hyphae. In merge image, red arrow showed two nuclei in a cell and green arrows represent empty cells without nuclear.

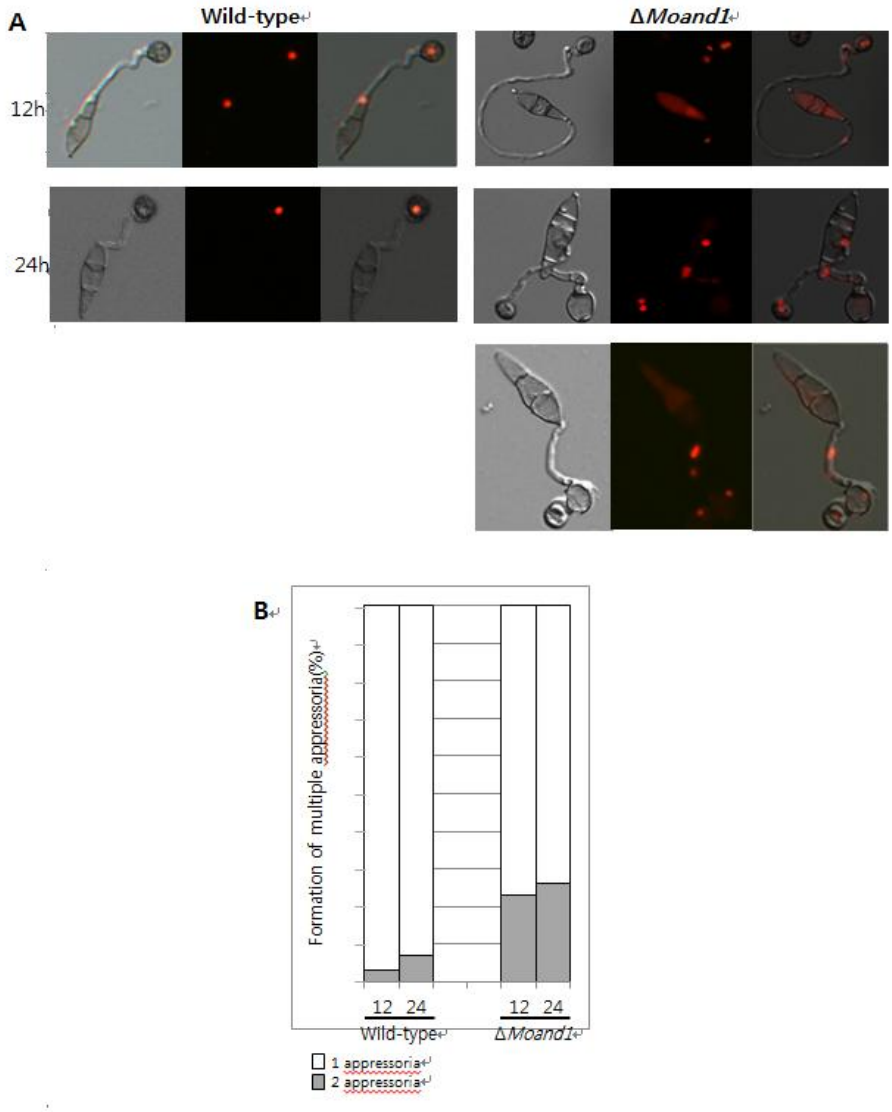

Figure 9. Formation of multiple appressoria.

(A) Conidial suspension was incubated on a coverslip to induce appressorial formation. The numbers of appressoria per conidium were measured after 12 and 24 hour of incubation.

(B) White portions of the bars represent the percentage of conidia that formed one appressorium, and grey portions represent the percentages of conidia that had two appressoria along with germ tubes.

Ⅶ. Pathogenicity and penetration of the Δ*Moand1* mutant

To determine the function of *MoAND1* in the plant infection, susceptible rice seedlings were sprayed with the Δ*Moand1* mutant, its complemented strain conidia and wild-type (Fig. 10). The wild-type developed typical necrotic lesions that mostly fused with other lesions, but Δ*Moand1* almost failed in disease development, only causing a few small necrotic lesions while Moand1c fully recovered the pathogenicity defect (Fig. 10). To characterize whether changes in pathogenicity in the Δ*Moand1* strain was due to defects in plant penetration and invasive growth, rice sheath tissues were inoculated with conidial suspension ($5X10^4$ conidia/ml). While the wild type penetrated into host cells through appressoria and developed invasive hyphae (Fig. 10), majority of appressoria in Δ*Moand1* penetrated only one cell. Their invasive growth appeared to be retarded (Fig. 10). Abnormalities in appressorium-mediated penetration and invasive growth of Δ*Moand1* were rescued by expression of *MoAND1* in the Moand1c strain. These results indicate that Δ*Moand1* mutant exhibit defects in penetration and invasive growth.

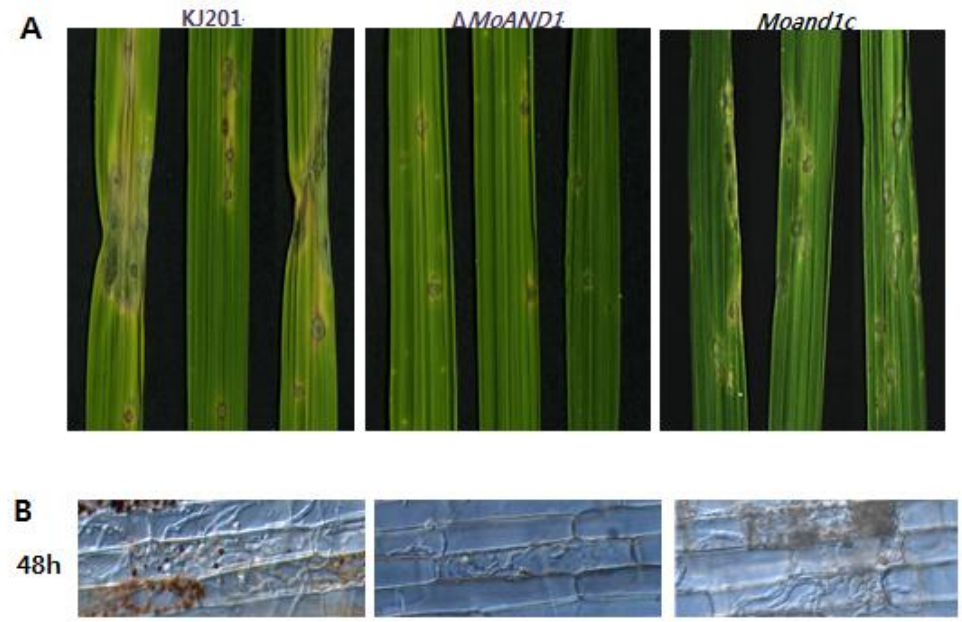

Figure 10. Pathogenicity and invasive growth of *MoAND1* in rice.

(A) Spray inoculation for pathogenicity assay of *MoAND1* deletion mutant. Susceptible rice seedlings were sprayed with conidia suspension of each strain and harvested at 7 day post inoculation.

(B) Leaf sheath injection of *MoAND1* deletion mutant. Excised rice leaves were injected with conidia suspension of wild-type and *MoAND1* deletion mutant. Infection hyphae were observed with light microscopic at 48 hours after incubation.

Ⅷ. Conidia viability of *⊿Moand1*

Δ*Moand1* showed significantly reduced germination and appressorium rate. To understand whether the conidia produced by Δ*Moand1* mutant were inherently defective in germination or they lose their viability quickly, the ability of conidia to germinate was examined. About 19% of 8-day-old Δ*Moand1* mutant conidia germinated, while 95% of conidia germinated in the wild-type strain. With increasing incubation time of conidial cultures, the frequency of conidial germination maintained to 92% in the wild-type strain, but the germination rates increased to 25% in Δ*Moand1* mutant. The frequency of conidial germination in Δ*Moand1* mutant was again decreased to 22%, while the wild-type strain maintained germination rates at a high level when conidia from 16-day-old culture plates were tested (Fig. 11). Since conidial germination rate of Δ*Moand1* maintained steadily, incubation time did not affect conidial viability. As shown in Figure. 11, wild-type conidia maintained their germination ability up to 4 days after incubation at 4℃. However, the number of viable conidia able to germinated decreased rapidly in the Δ*Moand1* mutant, and only 8% of their conidia germinated 4 days after incubation at 4℃. These results suggest that Δ*Moand1* mutant conidia become more susceptible at 4℃ stress and not in incubation time.

Conidia viability of Δ*Moand1* mutant was further confirmed by FUN-1 staining, the yeast viability stain that requires both plasma membrane integrity and metabolic capability to differentiate living and dead cells(Millard *et al.*, 1997). The 5% of defective conidia of *ΔMoand1* mutant were not stained with FUN-1(data not shown), while 95% of *ΔMoand1* conidia showed orange-red intravaculolar inclusions called cylindrical intravacuolar structures(CIVS) in metabolically active conidia same as wild-type conidia.

Conidia viability was also measured by staining dead cells with Phloxine B. Conidia were stained with 20ug/ml phloxine B for 1hr at room temperature. As control for dead cells, wild-type cells were incubated for 10min at 65℃. Although wild-type cells maintained original status, controls for dead cells (wild-type incubated at 65℃) showed pink colored conidia which means conidia lost their viability. In case of Δ*Moand1*, 97% of conidia showed viability as wild-type cells and only 3% of conidia lost their viability in conidia of Δ*Moand1*. These results suggest that deletion of *MoAND1* did not affect conidia viability.

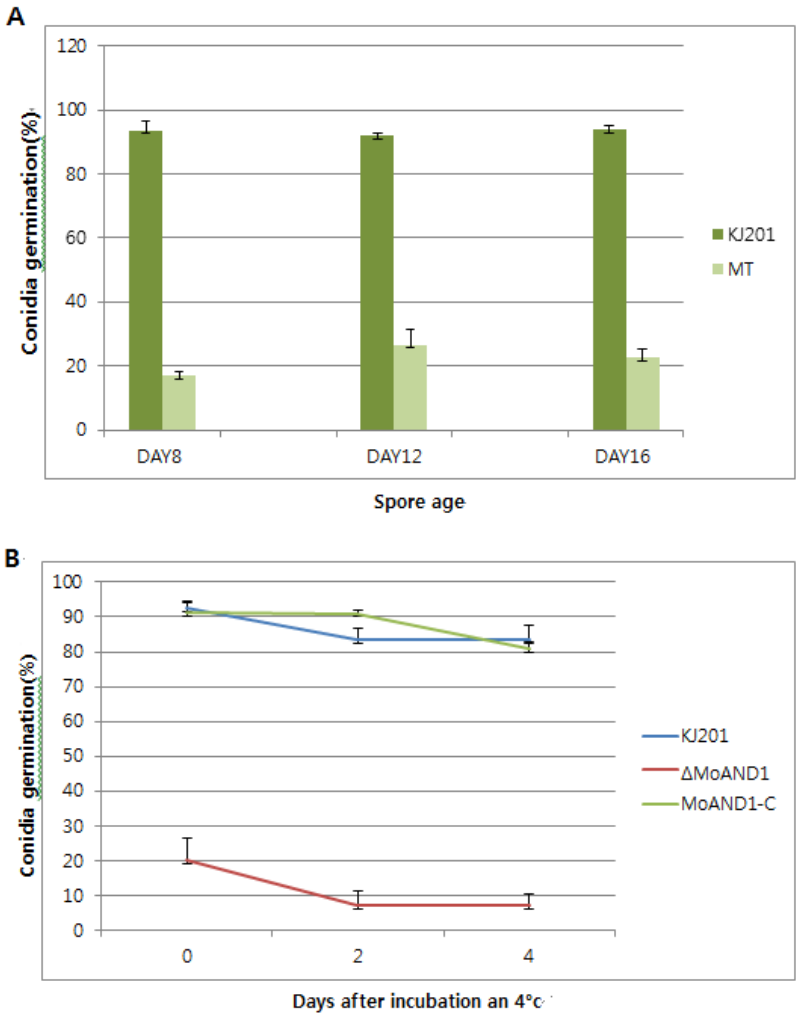

Figure 11. viability and germination of conidia formed by wild-type and *MoAND1* deletion mutant.

(A) Conidia were collected from indicated day-old cultures, and used in germination assays. (B) Conidia were collected from 12-day-old cultures, stored 4℃ and used in germination assays.

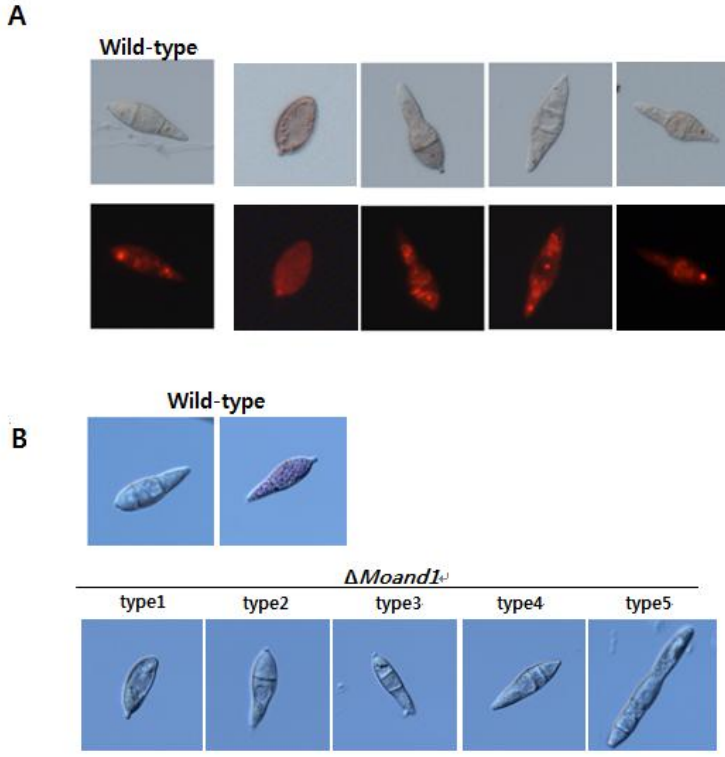

Figure 12. Viability test of Δ*Moand1*

(A) Ten-day-old conidia from wild-type and Δ*Moand1* mutant were stained with fluorescent dye FUN-1 (live/dead yeast viability stain). Conidia were observed by light or UV microscope. In dead cells, FUN-1 due to the loss of plasma membrane was depicted with ovoid.

(B) Ten-day-old conidia from wild-type and Δ*Moand1* mutant were stained with fluorescent dye Phloxine B. And also dead cells are stained by Phloxine B showing a pink color.

Ⅸ. Double KO mutant of *MoAND1* and *MoAND2*

To find relationship between *MoAND1* and *MoAND2*, double KO mutant was constructed. Usually, the phenotype of the double mutants could be mainly predicted from the phenotypes of the single mutants, interesting interaction and more precise gene action can be revealed by double KO. The double KO mutant of *MoAND1* and *MoAND2* was produced by using targeted gene replacement method as described before. For double KO mutant, the *MoAND2* gene deletion vector constructs were transformed into protoplasts of *MoAND1* deletion mutant (Fig. 13). In the Double KO mutant, conidia morphology was similar with Δ*Moand1* mutant, but hyphal growth was severely affected in complement and minimal agar media as shown in Figure 14. Especially, in minimal agar media, hyphal growth of double mutant reduced about three times compared with wild-type. Moreover, pathogenicity was significantly reduced since double KO mutant showed significantly reduced germination and appressorium rate and more importantly appressorium of double KO mutant did not penetrate tissue surface of rice causing loss of pathogenicity (Fig.15). Taken together, these results indicated that deletion of *MoAND1* and *MoAND2* caused more severe cellular mechanisms of developmental stages such as hyphal growth, germination and pathogenicity.

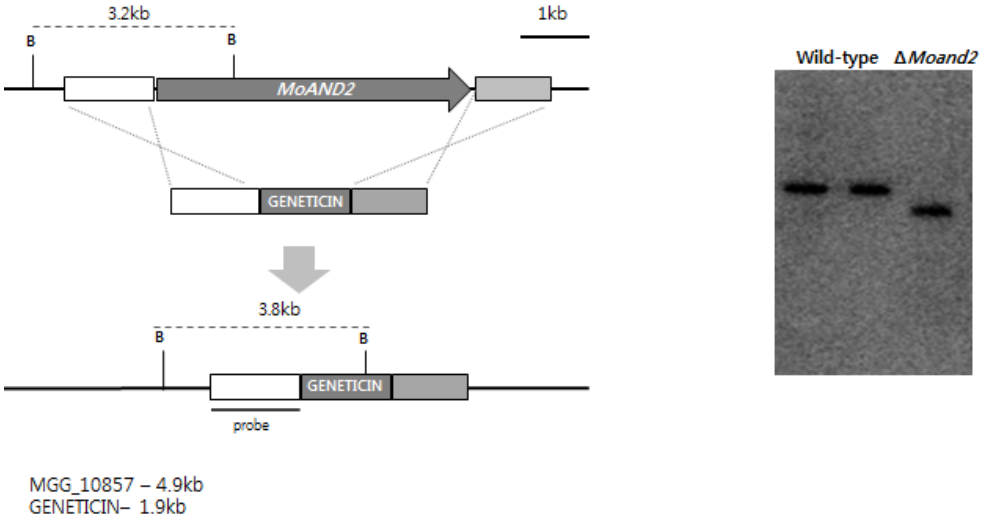

Figure 13. Targeted gene replacement for double KO in *M. oryzae*.

Schematic diagram of targeted gene replacement. *MoAND2* gene ORF (arrow) was replaced with *GENETICIN* cassette in background of *MoAND1* gene deletion protoplast. Restriction enzyme site and flanking region (white and light gray box) is shown above the lines representing genomic regions spanning target loci. To confirm the deletion mutants, Southern hybridization was performed. Each band size was identified using flanking region as probe.

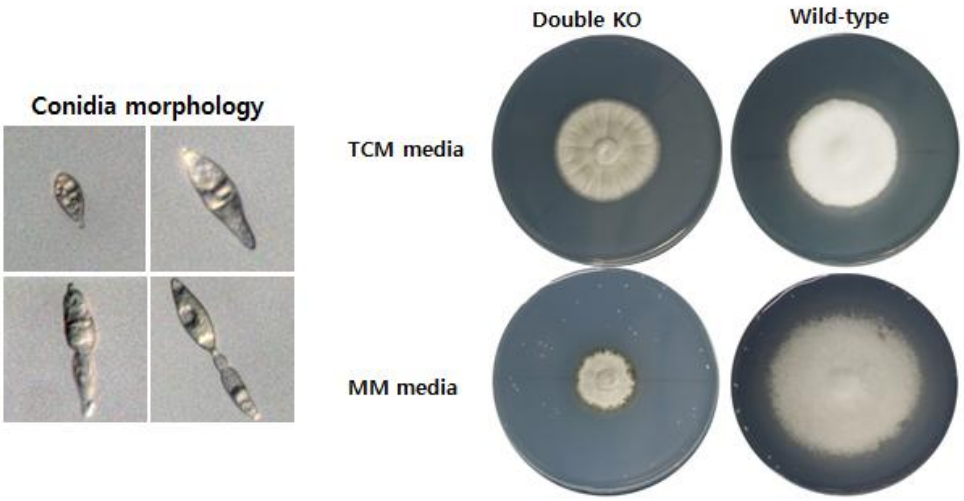

Figure 14. Characterization of developmental characteristics in wild-type, Δ*Moand1* and double KO mutant.

(A) Conidia obtained from 7-day-old cultures grown on oatmeal agar plates and conidia shapes were observed under a light microscope

(B) Growth rate was measured in wild-type and double KO mutant in Complement agar and Minimal agar from 10-days-old media.

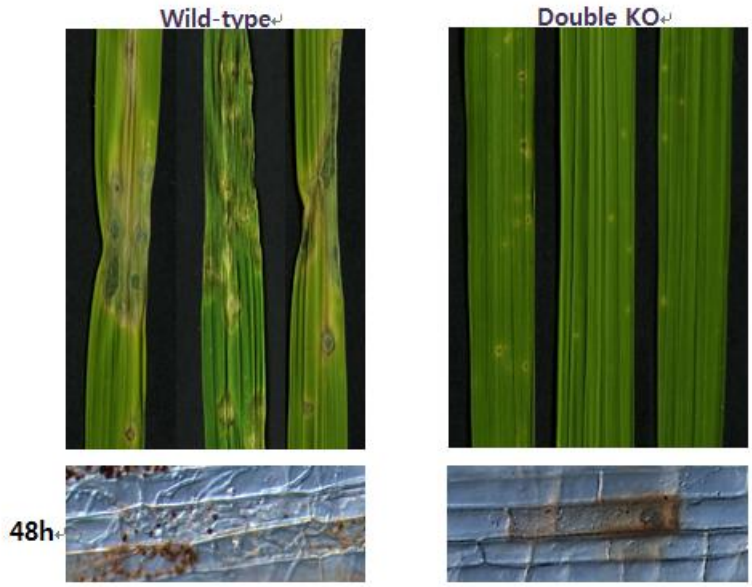

Figure 15. Pathogenicity and invasive growth Double KO mutant in rice.

(A) Spray inoculation for pathogenicity assay of Double KO mutant. Susceptible rice seedlings were sprayed with conidia suspension of each strains and harvested at 7 day post inoculation.

(B) Leaf sheath injection of Double KO mutant. Excised rice leaves were injected with conidia suspension of wild-type and Double KO mutant. Infection hyphae were observed with light microscopic at 48 after incubation.

Ⅹ. Benomyl resistance of wild-type, Δ*Moand1* and Double KO mutant.

The observed phenotypes in Δ*Moand1* and Double KO mutants suggested possibility that defects of microtubule functions same as homologous genes such as *ApsA and ApsB* in *Aspergillus nidulans* or *Mcp5* and *Mcp6* in *Schzoscharromyces pombe*. It is well known a fact that mutants are defective in microtubule function often sensitive to microtubule-depolymerizing agents such as Benomyl. We determined resistance to benomyl by culturing onto complement agar media containing 0.5ug/ml concentration of the inhibitor. Indeed, growth of Double KO mutant was more sensitive than wild-type, although less so than Δ*Moand1* mutant. Interestingly, Δ*Moand1* showed significantly reduced growth pattern and only 30% growth of Δ*Moand1* was restored. From these results, it can be explained that the phenotypes of abnormal nuclear distribution in conidia, hyphae and even appressorium in Δ*Moand1* and Double KO mutant caused by defects of microtubules subsequently affecting nuclear migration in development stages.

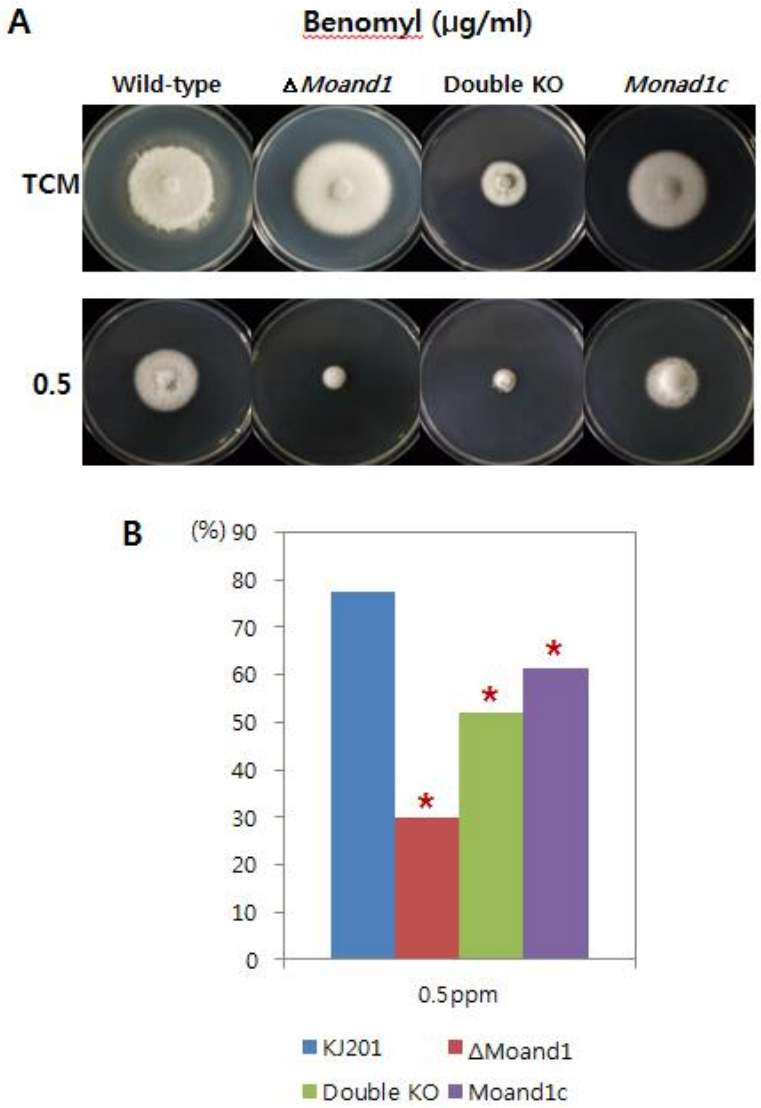

Figure 16. Benomyl resistance of wild-type, Δ*Moand1* and Double KO mutant.

(A) Each type of strains was cultured on Complement agar media containing the concentration of Benomyl indicated. Plates were incubated for 10 days. (B) Growth pattern was represented by graph with percentages of growth compared with wild-type.

Table 1. Oligo sequences used in this study

Name	Sequence (5' → 3')
HPH_F	GGCTTGGCTGGAGCTAGTGGAGG
HPH_R	GTTGGTGTCGATGTCAGCTCCGGAG
MGG_02961.6_UF	GCTTTTGGGACTACTGTTGTTCGC
MGG_02961.6_UR	CGGCGACCATCA AGCGTGTTT
MGG_02961.6_DF	CGACATTCGCTCAACCATTCTTTCACA
MGG_02961.6_DR	GCTGGGCGGAGTTCTTTTCAATGG
MGG_02961.6_NST_F	ACGAGGCGCCACATGAT
MGG_02961.6_NST_R	GGGAGGCGGCTGTAGTAAGTATCA T
MGG_02961.6_qRT_F	GTTGGTCGGTCAGAGGCAAGG
MGG_02961.6_qRT_R	GAACTTGATAGCACGGCCGG
MGG_10857.6_UF	ACAGCCTCATGAAAACCGGACG
MGG_10857.6_UR	CGGGACAAATGACGCGCTCG
MGG_10857.6_DF	CAACCGCTACTGACCCCACC
MGG_10857.6_DR	AGGAGGGCCGACTAGAACAG
MGG_10857.6_NST_F	TGGACCACTCACAGGACGTTGC
MGG_10857.6_NST_R	GTCCCAGACCCCAAGACCAG
MGG_10857.6_qRT_F	GTCCTTCACCCAGCATACCGA
MGG_10857.6_qRT_R	GCTCCGGTCCTGTACTCGC

DISCUSSTION

Eukaryotes possess a wide variety of conserved nuclear migration systems by microtubule related proteins, but the functions of these proteins were not identified across different species. In the course of our study to determine the molecular mechanism(s) underlying nuclear migration in *M. oryzae*, *MoAND1* and *MoAND2*, were identified and characterized. In *Aspergillus nidulans*, the ApsA and ApsB proteins which are homologous to *MoAND1* and *MoAND2* in *M. oryzae*, affect nuclear migration by defecting astral and cytoplasmic microtubules (Fischer & Timberlake, 1995), (Suelmann *et al.*, 1998). Mutations in *A.nidulans ApsA* lead to curved and thinner microtubules and in *ApsB* mutation showed reduction of astral microtubules affecting abnormal nuclear migration and positioning. In Saccharomyces *cerevisiea*, Num1 protein affects nuclei migration. Moreover, microtubule forces are involved in anchoring the nucleus at bud neck and in early stages of nuclear elongation through the neck (Kormanec *et al.*, 1991). As shown the results before, function of MoAND1 protein could explained if we assume that *MoAND1* serves a similar function as *ApsA* in *Aspergillus nidulans*. ApsA interacts with MT-plus end localized dynein is activated, it tugs at MTs and pulls attached nuclei. The situation could

similar in *M. oryzae* where MoAND1 could serve as a docking place for microtubules. In *MoAND1* deletion mutant, the contact might not be established and nuclear migration was affected. This can be proved by benomyl compounds that promote microtubule depolymerization and reflect the intrinsic stability of cellular microtubules (Cottingham & Hoyt, 1997). In benomyl media, growth of *MoAND1* deletion mutant and double KO mutant of *MoAND1* and *MoAND2* were more severely affected compared with wild-type. This phenomenon usually showed in mutants that are defective in function of microtubules.

Unlike other organisms such as *A. nidulas*, *S. cerevisiae*, nuclear migration and positioning is especially important to a plant pathogenic fungus, *M. oryzae* for development specialized structure called appressoria. Previous analysis has shown that development of appressoria in the rice blast fungus requires a morphogenetic program regulated by the cAMP response pathway and the Pmk1 MAK kinase cascade in response to the hard, hydrophobic rice leaf surface(Dean, 1997),(Wilson & Talbot, 2009). In response to these signals, a germinating conidium undergoes a single round of mitosis, which is a necessary prerequisite for appressorium differentiation (Veneault-Fourrey et al., 2006).

We have found that deletion of *MoAND1* causes pleotropic phenotypes spanning *M. oryzae* development: namely conidial morphology, appressorium formation and invasive growth. Each of these features contributes to pathogenic fitness. Normal shape of three-celled conidia affects proper germination development on hydrophobic surface of host cell. It is conceivable that the abnormal conidial morphology in *MoAND1* deletion mutant predominantly blocks subsequent development of conidial germination, because nuclei were absent or abnormally distributed in conidia cells. After conidia germination, successful appressoria formation is essential for pathogenicity. In this study, we showed that *MoAND1* deletion mutant and double KO mutant of *MoAND1* and *MoAND2* are incapable of producing functional appressoria. In *MoAND1* deletion mutant and double KO mutant of *MoAND1* and *MoAND2,* conidia formed a germ tube and appressorium developed a second germ tube and appressorium at the same or opposite orientation, and subsequently a third, having total of three appressoria. These results caused by abnormal nuclear distribution at conidia and germ tube in *MoAND1* deletion mutant and double KO mutant. In these mutants, only about 30% and 50% appresorria from germinated conidia was produced respectively but penetration to rice surface was unsuccessful.

MoAND1 deletion mutant showed slower hyphal growth and invasive growth *in planta* resulting only a few invasive growths successfully moved next cells. Moreover, in double KO mutant, appressoria even penetrate host cell surface resulting significantly reduced pathogenicity.

Together, these results suggest that further studies characterizing *MoAND1* and *MoAND2* mediated regulation of nuclear movement well help to dissect the evolutionary mechanisms underlying these key processes, potentially leading to novel strategies for crop protection.

LITERATURE CITED

Brachat, A., J. V. Kilmartin, A. Wach & P. Philippsen, (1998) *Saccharomyces cerevisiae* cells with defective spindle pole body outer plaques accomplish nuclear migration via half-bridge-organized microtubules. *Mol. Biol. Cell* **9**: 977-991.

Chi, M. H., S. Y. Park & Y. H. Lee, (2009) A Quick and Safe Method for Fungal DNA Extraction. *Plant Pathology J* **25**: 108-111.

Choi, J., Y. Kim, S. Kim, J. Park & Y. H. Lee, (2009) MoCRZ1, a gene encoding a calcineurin-responsive transcription factor, regulates fungal growth and pathogenicity of *Magnaporthe oryzae*. *Fungal Genet. Biol.* **46**: 243-254.

Cottingham, F. R. & M. A. Hoyt, (1997) Mitotic spindle positioning in Saccharomyces cerevisiae is accomplished by antagonistically acting microtubule motor proteins. *The Journal of cell biology* **138**: 1041-1053.

Dean, R. A., (1997) Signal pathways and appressorium morphogenesis. *Annu. Rev. Phytopathol.* **35**: 211-234.

Fischer, R. & W. E. Timberlake, (1995) *Aspergillus nidulans* apsA (anucleate primary sterigmata) encodes a coiled-coil protein required for nuclear positioning and completion of asexual development. *The Journal of*

cell biology **128**: 485-498.

Kim, S., S. Y. Park, K. S. Kim, H. S. Rho, M. H. Chi, J. Choi, J. Park, S. Kong, J. Park, J. Goh & Y. H. Lee, (2009) Homeobox Transcription Factors Are Required for Conidiation and Appressorium Development in the Rice Blast Fungus *Magnaporthe oryzae*. *PLoS Genet.* **5**.

Koga, H., K. Dohi, O. Nakayachi & M. Mori, (2004) A novel inoculation method of *Magnaporthe grisea* for cytological observation of the infection process using intact leaf sheaths of rice plants. *Physiol. Mol. Plant Pathol.* **64**: 67-72.

Kormanec, J., I. Schaaffgerstenschlager, F. K. Zimmermann, D. Perecko & H. Kuntzel, (1991) Nuclear migration in *Saccharomyces cerevisiae* is controlled by the highly repetitive 313 kDa NUM1 protein. *Mol. Gen. Genet.* **230**: 277-787.

Lau, G. W. & J. E. Hamer, (1998) *Acropetal*: A genetic locus required for conidiophore architecture and pathogenicity in the rice blast fungus. *Fungal Genetics and Biology* **24**: 228-239.

McGinnis, S. & T. L. Madden, (2004) BLAST: at the core of a powerful and diverse set of sequence analysis tools. *Nucleic Acids Res.* **32**: W20-W25.

Millard, P. J., B. L. Roth, H. P. Thi, S. T. Yue & R. P. Haugland, (1997)

Development of the FUN-1 family of fluorescent probes for vacuole labeling and viability testing of yeasts. *Appl. Environ. Microbiol.* **63**: 2897-2905.

Mulder, N. J., R. Apweiler, T. K. Attwood, A. Bairoch, A. Bateman, D. Binns, P. Bradley, P. Bork, P. Bucher, L. Cerutti, R. Copley, E. Courcelle, U. Das, R. Durbin, W. Fleischmann, J. Gough, D. Haft, N. Harte, N. Hulo, D. Kahn, A. Kanapin, M. Krestyaninova, D. Lonsdale, R. Lopez, I. Letunic, M. Madera, J. Maslen, J. McDowall, A. Mitchell, A. N. Nikolskaya, S. Orchard, M. Pagni, C. P. Pointing, E. Quevillon, J. Selengut, C. J. A. Sigrist, V. Silventoinen, D. J. Studholme, R. Vaughan & C. H. Wu, (2005) InterPro, progress and status in 2005. *Nucleic Acids Res.* **33**: D201-D205.

Park, J., B. Park, K. Jung, S. Jang, K. Yu, J. Choi, S. Kong, J. Park, S. Kim, H. Kim, S. Kim, J. F. Kim, J. E. Blair, K. Lee, S. Kang & Y. H. Lee, (2008) CFGP: a web-based, comparative fungal genomics platform. *Nucleic Acids Res.* **36**: D562-D571.

Reeve, W. J. & F. P. Kelly, (1983) Nuclear position in the cells of the mouse early embryo. *J. Embryol. Exp. Morphol.* **75**: 117-139.

Rogers, S. O. & A. J. Bendich, (1985) Extraction of DNA from Milligram Amounts of Fresh, Herbarium and Mummified Plant-Tissues. *Plant Mol. Biol.* **5**: 69-76.

Sambrook, J., E. F. Fritsch & T. Maniatis, (1989) *Molecular cloning: A laboratory manual.* Cold Spring Harbor Laboratory Press, Cold Spring Harbo, New York.

Saunders, D. G., Y. F. Dagdas & N. J. Talbot, (2010) Spatial uncoupling of mitosis and cytokinesis during appressorium-mediated plant infection by the rice blast fungus *Magnaporthe oryzae*. *The Plant cell* **22**: 2417-2428.

Suelmann, R., N. Sievers, D. Galetzka, L. Robertson, W. E. Timberlake & R. Fischer, (1998) Increased nuclear traffic chaos in hyphae of *Aspergillus nidulans*: molecular characterization of apsB and in vivo observation of nuclear behaviour. *Mol. Microbiol.* **30**: 831-842.

Talbot, N. J., D. J. Ebbole & J. E. Hamer, (1993) Identification and Characterization of Mpg1, a Gene Involved in Pathogenicity from the Rice Blast Fungus *Magnaporthe-Grisea*. *Plant Cell* **5**: 1575-1590.

Thompson, J. D., D. G. Higgins & T. J. Gibson, (1994) Clustal-W - Improving the Sensitivity of Progressive Multiple Sequence Alignment through Sequence Weighting, Position-Specific Gap Penalties and Weight Matrix Choice. *Nucleic Acids Res.* **22**: 4673-4680.

Valent, B., L. Farrall & F. G. Chumley, (1991) *Magnaporthe-Grisea* Genes for Pathogenicity and Virulence Identified through a Series of

Backcrosses. *Genetics* **127**: 87-101.

Veith, D., N. Scherr, V. P. Efimov & R. Fischer, (2005) Role of the spindle-pole-body protein ApsB and the cortex protein ApsA in microtubule organization and nuclear migration in *Aspergillus nidulans*. *J. Cell Sci.* **118**: 3705-3716.

Veneault-Fourrey, C., M. Barooah, M. Egan, G. Wakley & N. J. Talbot, (2006) Autophagic fungal cell death is necessary for infection by the rice blast fungus. *Science* **312**: 580-583.

Wilson, R. A. & N. J. Talbot, (2009) Under pressure: investigating the biology of plant infection by *Magnaporthe oryzae*. *Nat Rev Microbiol* **7**: 185-195.

Yu, J. H., Z. Hamari, K. H. Han, J. A. Seo, Y. Reyes-Dominguez & C. Scazzocchio, (2004) Double-joint PCR: a PCR-based molecular tool for gene manipulations in filamentous fungi. *Fungal genetics and biology : FG & B* **41**: 973-981.

요약(국문초록)

벼 도열병균은 생활사 동안 기주 식물과의 상호작용을 통해 다양한 형태학적 변이를 겪게 되어 상호작용의 메커니즘을 연구하는 대에 모델 병원균이다. 도열병균이 식물에 병을 내기 위한 침입기구인 Appressorium을 만들 때에 핵 이동 및 분포가 매우 중요한 과정이라는 것이 선행연구를 통해 밝혀져 있다. 본 연구에서는 벼 도열병균의 핵 이동에 관여하는 유전자의 연구를 위해 두 개의 *MoAND1*, *MoAND2* 유전자를 선발하였고, 이들의 기능적 특성을 규명하기 위하여 gene deletion mutant를 확보하였다. 두 유전자는 각각 *MoAND1* (*M. oryzae* Abnormal Nuclear Distribution1) 과 *MoAND2* (*M. oryzae* Abnormal Nuclear Distribution2)라 명명하였다. *MoAND1*과 *MoAND2*의 mutant를 이용한 기능분석에 따르면, 두 유전자는 conidia morphology에 중요한 역할을 하며, conidia에서 핵의 분포도 역할을 하였다. *MoAND1 결손 변이체는* 핵 뿐만 아니라, 균사에서도 핵이 비정상적으로 분포하는 것으로 나타났고, 핵이 존재하지 않는 빈 세포도 발견되었다. 또한, germination 비율이 줄어들어, appressorium 형성률이 감소하게 되었고 이로 인해, invasive growth가 줄어들어 병원성이 감소하였다. 또한, *MoAND1 결손 변이체는*, *MoAND1* and *MoAND2* double KO 군주에서는 모두 microtubules depolyzing Benomyl에 더 민감하게 반응함에 따라 위에서 나타난 비정상적인 핵 이동의 원인이 microtubule의 기능 이상에 기인함을 증명할 수 있었다.

따라서, 본 연구에서 기능 분석한 두 핵 이동 유전자에 대한 연구 결과는 병 발생에 있어 중요한 역할을 규명한 것으로 판단되어 석사학위논문으로 충분한 가치가 있다고 여겨진다.

주요어 : 벼 도열병균, 핵 이동

학 번 : 2011-21275